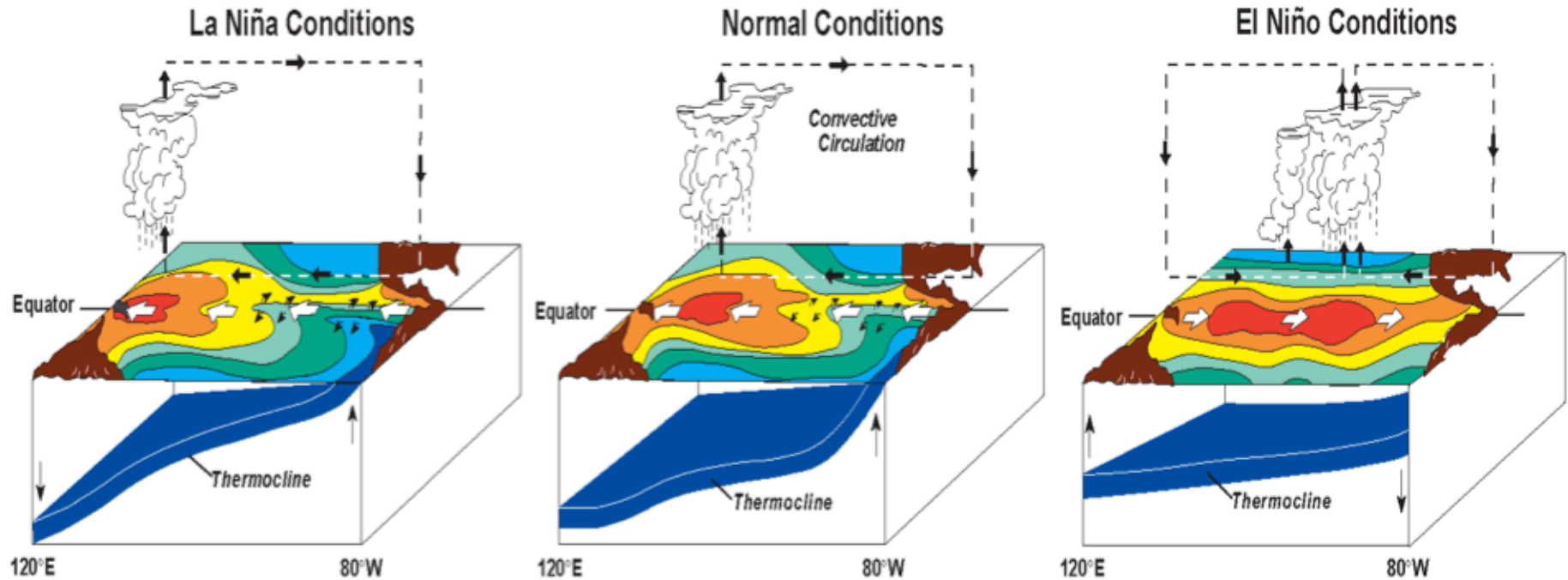


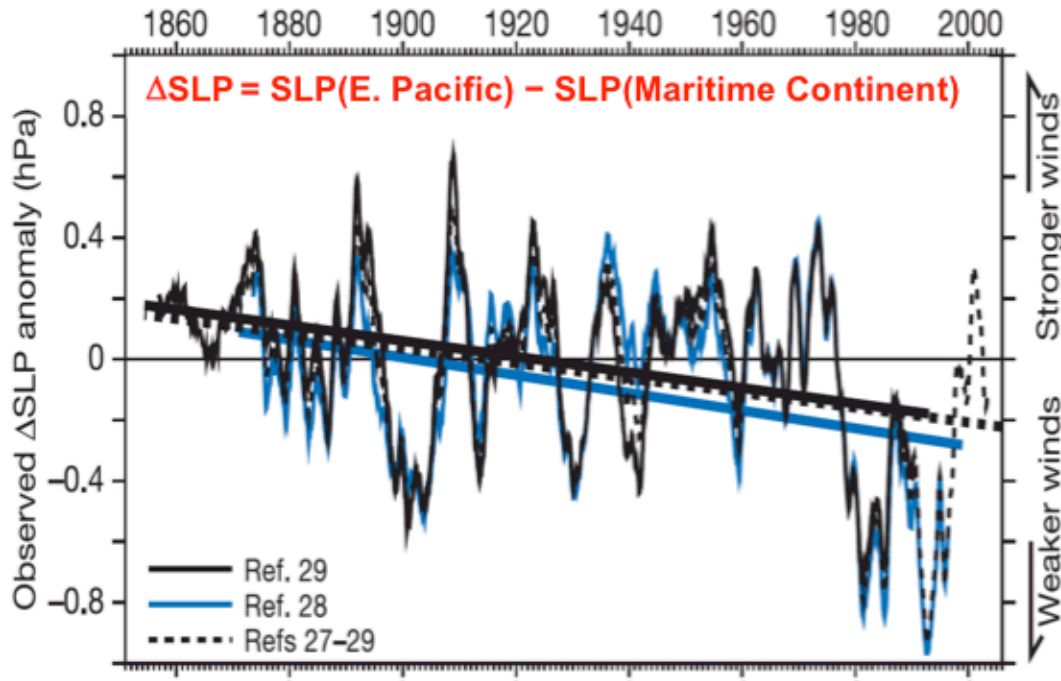
Role of the stability in the Bjerknes feedback for the recent change in the Walker circulation

B.J. Sohn, Seoul National University, Korea
(with Sukyoung Lee, Penn State)

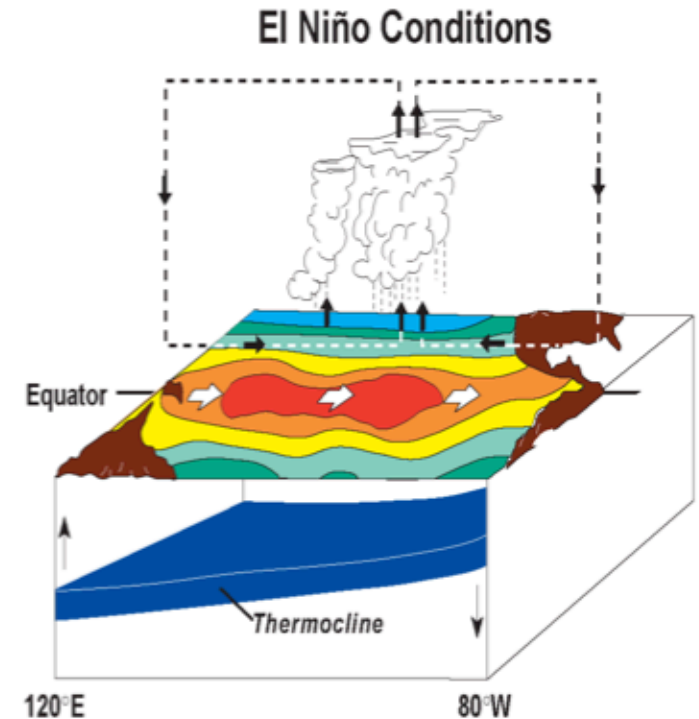
Variation of Pacific Walker circulation (PWC) (Bjerknes feedback)



More El Niño condition under the global warming



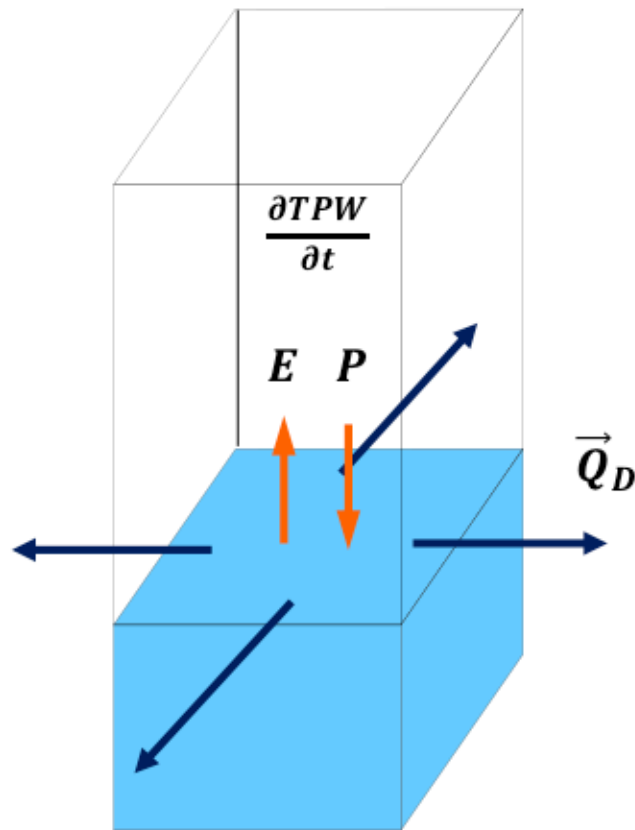
Vecchi et al. (2006, Nature)



- Weakening of the Walker circulation since mid 19th century.
- Largely due to anthropogenic forcing.
- Further weakening of tropical atmospheric circulation during the 21st century.

Water vapor transport from satellite/reanalysis data

Examining Walker circulation change from satellite/reanalysis-derived water vapor transport



Satellite (HOAPS)

$$\frac{\partial TPW}{\partial t} + \nabla \cdot \vec{Q} = E - P$$

$E - P$ = Evaporation - Precipitation

$$\vec{Q} = \vec{Q}_R + \vec{Q}_D$$

\vec{Q}_R : Rotational component

\vec{Q}_D : Divergent component

$$\nabla \cdot \vec{Q}_D = E - P - \frac{\partial TPW}{\partial t} = -\nabla^2 \Phi \quad \Rightarrow \quad \vec{Q}_D = \nabla \Phi$$

Reanalysis & Model outputs

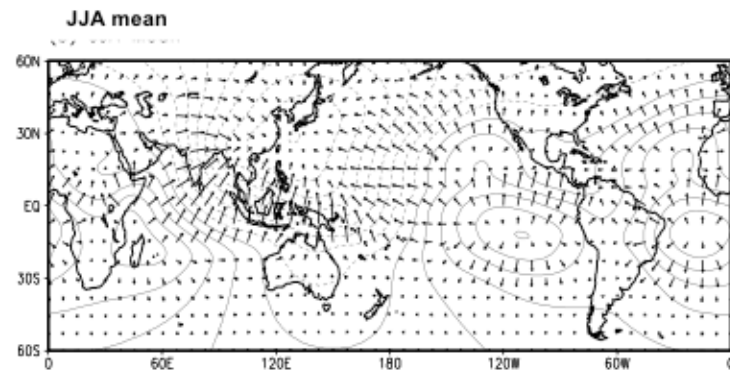
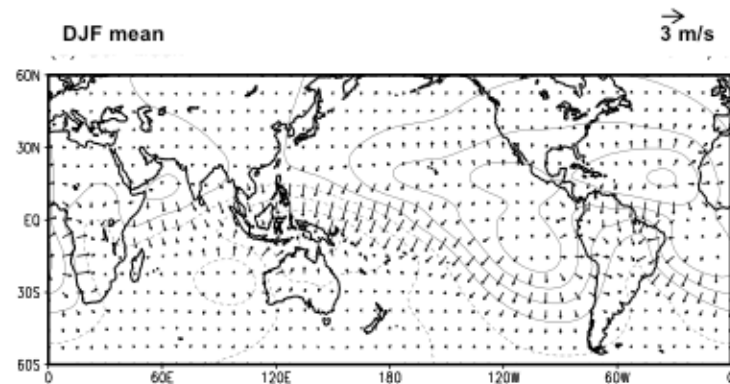
$$\vec{Q} = -\frac{1}{g} \int_{p_s}^0 q \vec{V} dp$$

Effective wind for vapor transport (\vec{V}_E)

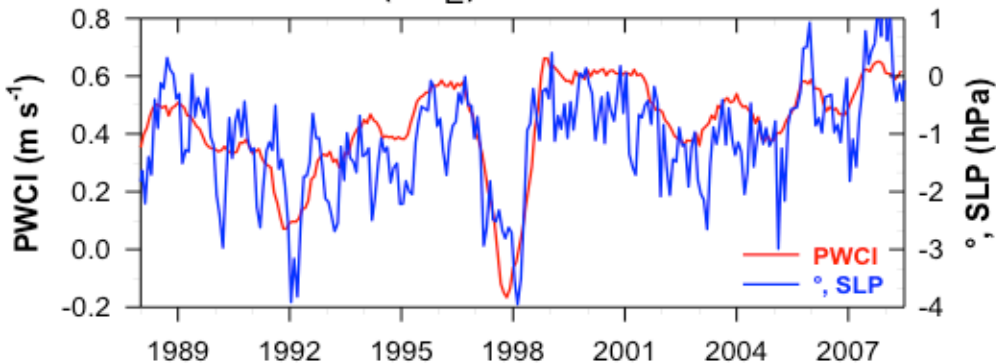
$$\begin{aligned}\vec{Q}_D &= \frac{1}{g} \int_{p_s}^0 q \vec{V}_D dp \\ &= \vec{V}_E \cdot \frac{1}{g} \int_{p_s}^0 q dp = \vec{V}_E \cdot TPW(t)\end{aligned}$$

$$\vec{V}_E = \frac{\vec{Q}_D}{TPW} : \text{Effective wind}$$

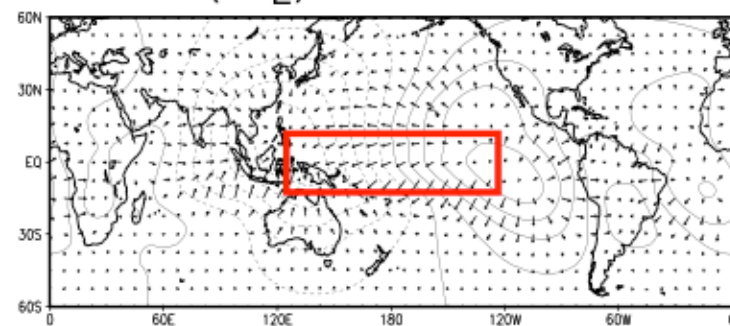
ERA40 Effective wind



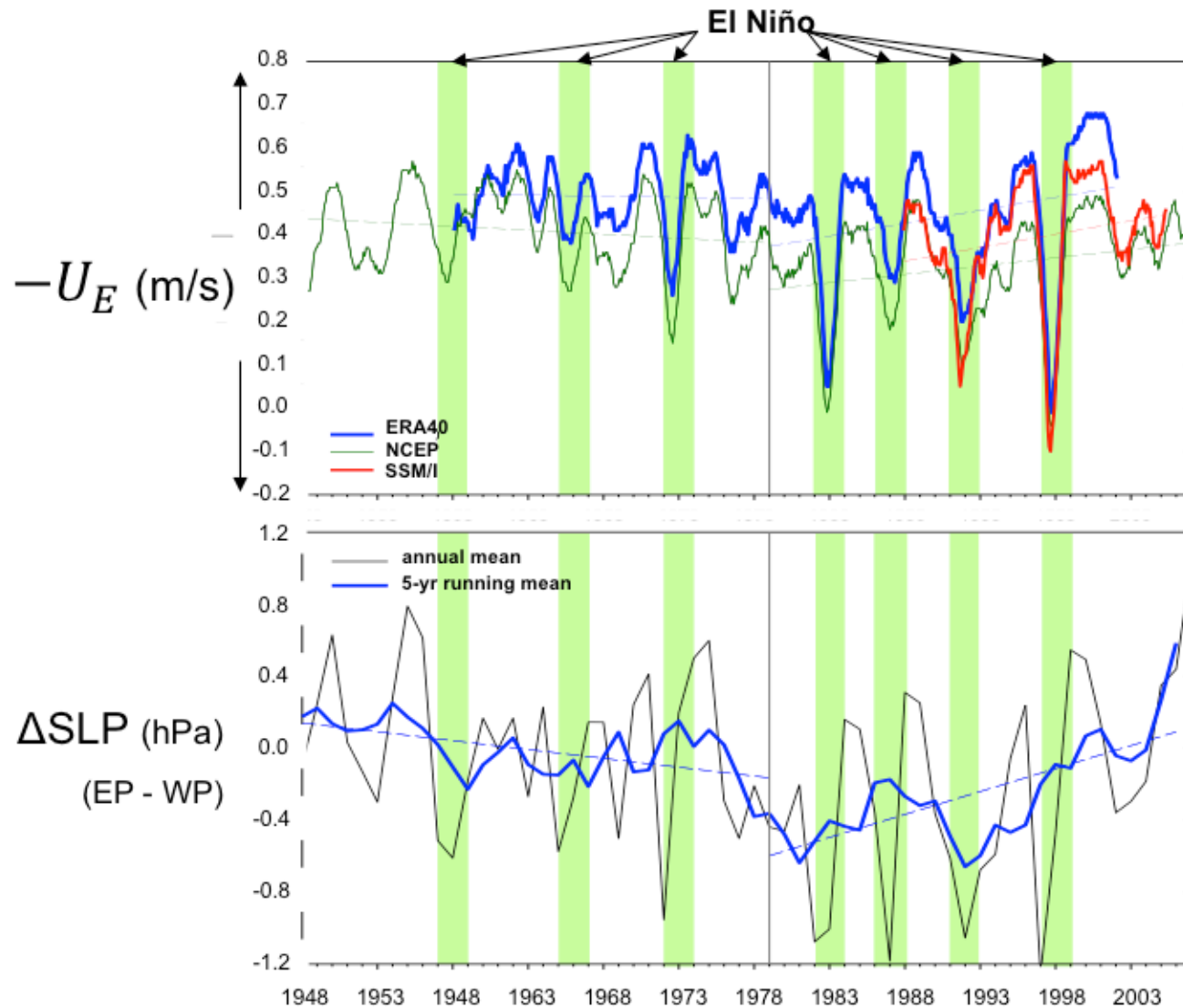
PWCI ($-U_E$) vs. Δ SLP



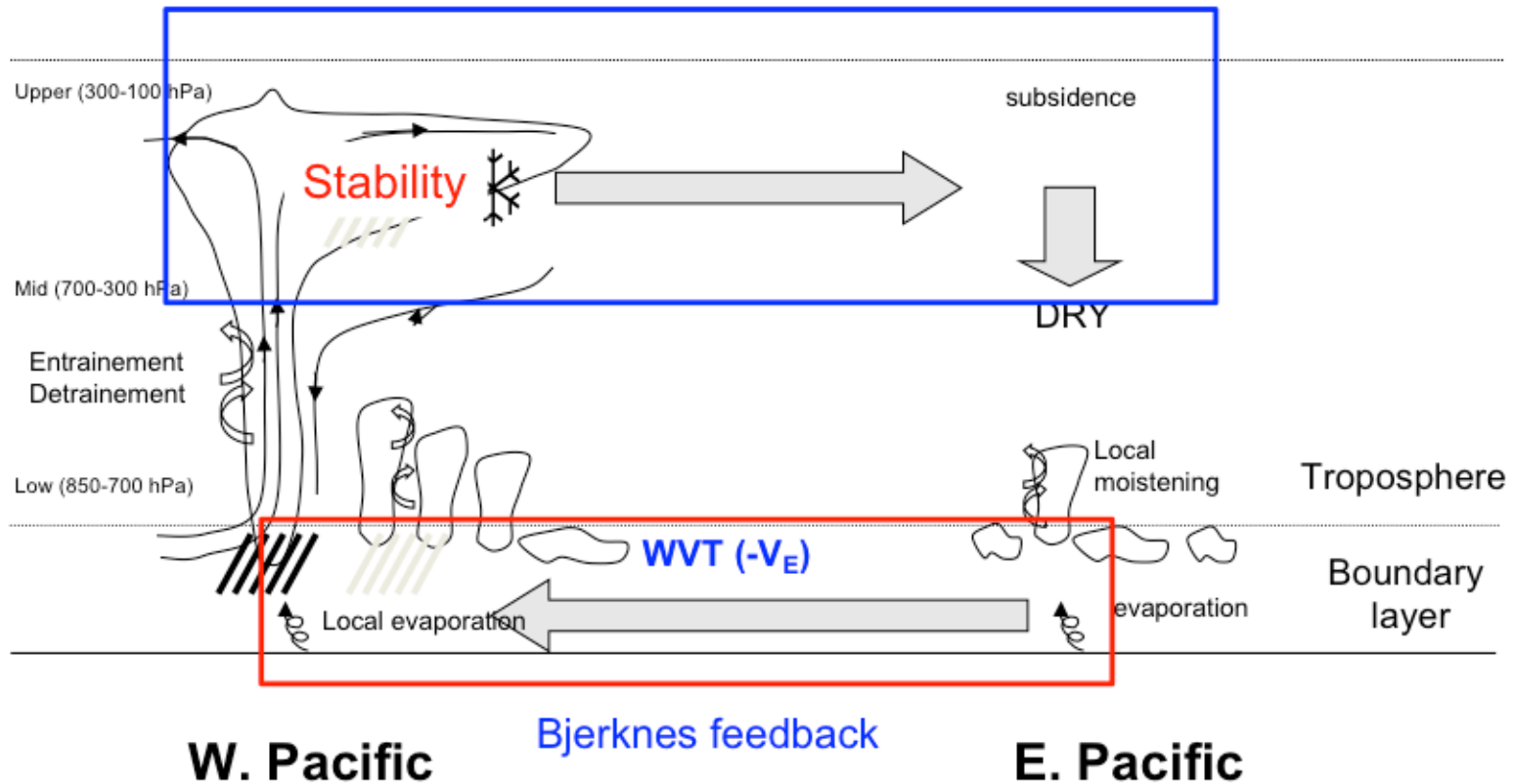
PWCI ($-U_E$)



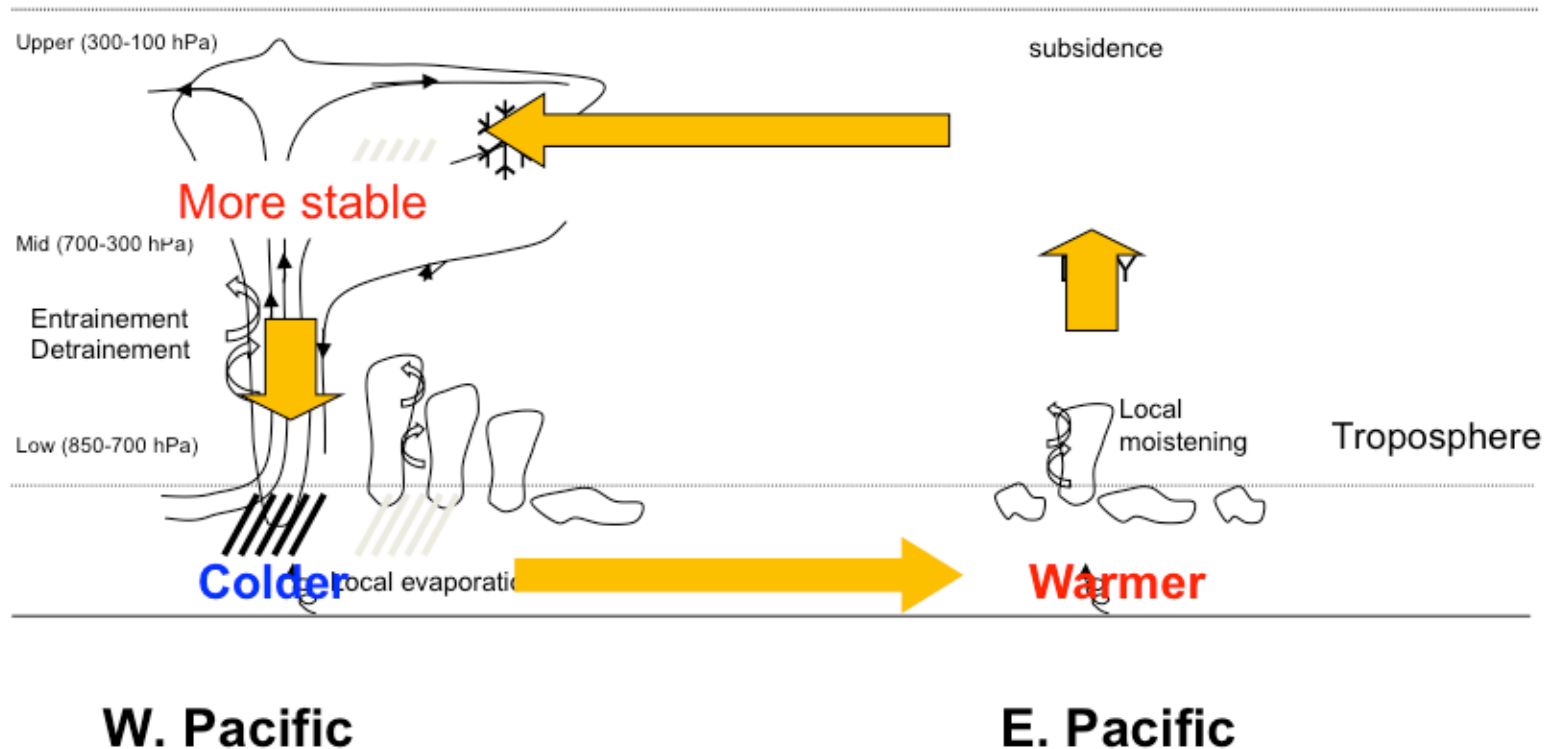
Pacific Walker circulation index ($-U_E$)



Stability role in the Walker circulation?



More stable conditions in current models

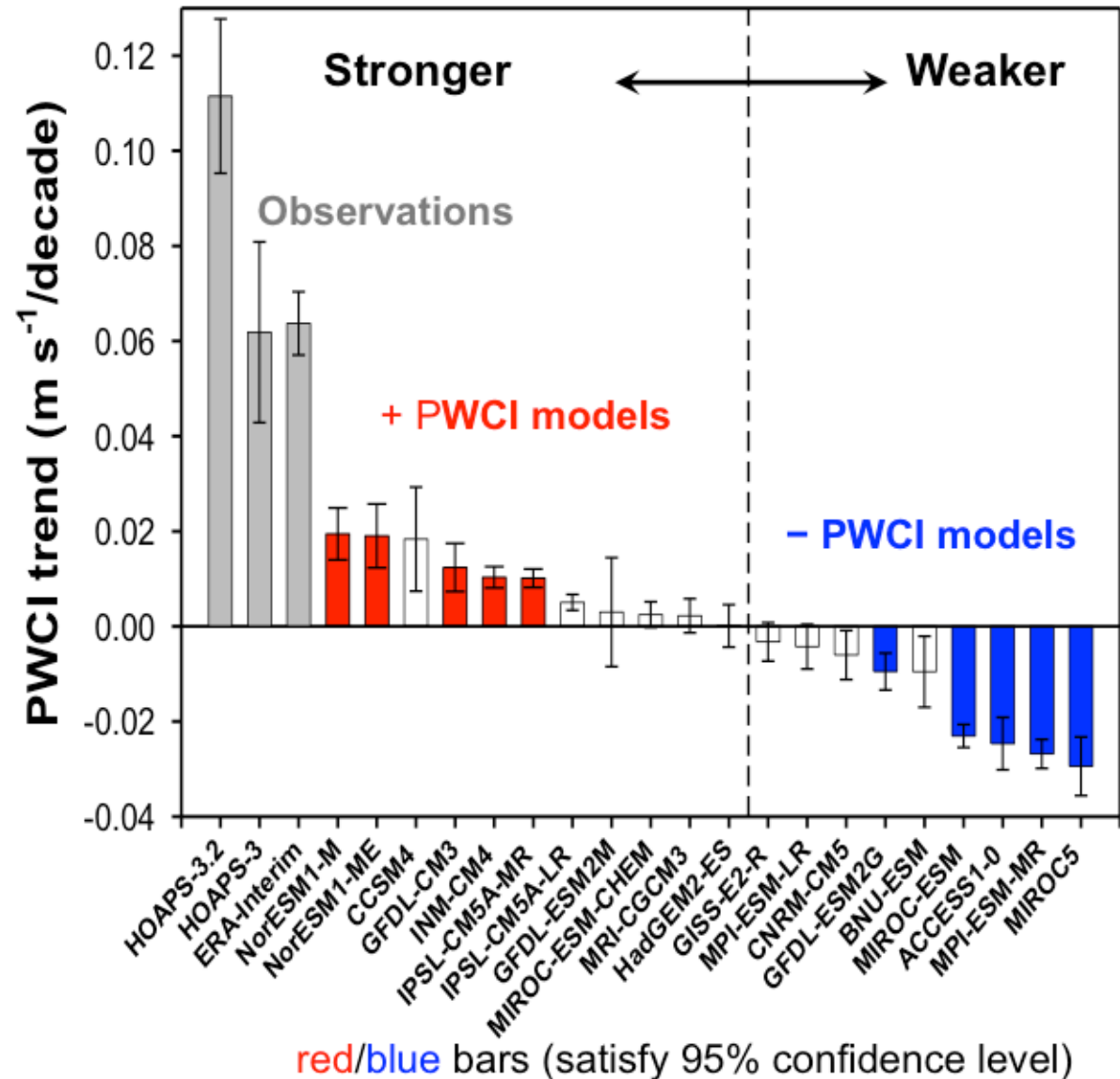


PWCI trends (Observation, Reanalysis, and CMIP5)

Period : 1979–2012

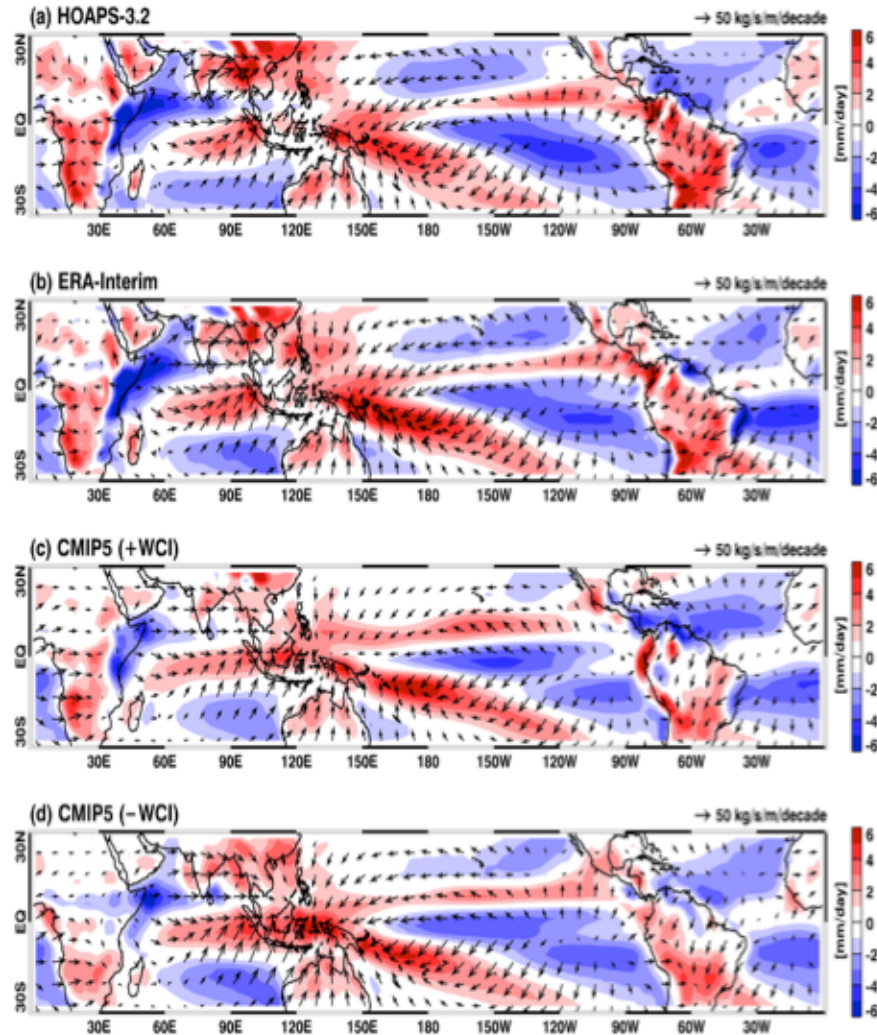
20 CMIP5 models (Historical + RCP4.5), r1i1p1

- GFDL-CM3 (USA): 144×90×23
- INM-CM4 (Russia): 180×120×17
- IPSL-CM5A-MR (France): 144×143×17
- NorESM1-M (Norway): 144×96 ×17
- NorESM1-ME (Norway): 144×96×17
- ACCESS1-0 (Australia): 192×144×17
- GFDL-ESM2G (USA): 144×90×17
- MIROC5 (Japan): 256×128×17
- MIROC-ESM (Japan): 128×64×35
- MPI-ESM-MR (Germany): 192×96×25
- BNU-ESM (China): 128×64×17
- CCSM4 (USA): 288×192×17
- CNRM-CM5 (France): 256×128×17
- GFDL-ESM2M (USA): 144×90×17
- GISS-E2-R (USA): 144×90×17
- HadGEM2-ES (UK): 192×144×17
- IPSL-CM5A-LR (France): 96×96×17
- MIROC-ESM-CHEM (Japan): 128×64×35
- MPI-ESM-LR (Germany): 192×96×25
- MRI-CGCM3 (Japan): 320×160×23

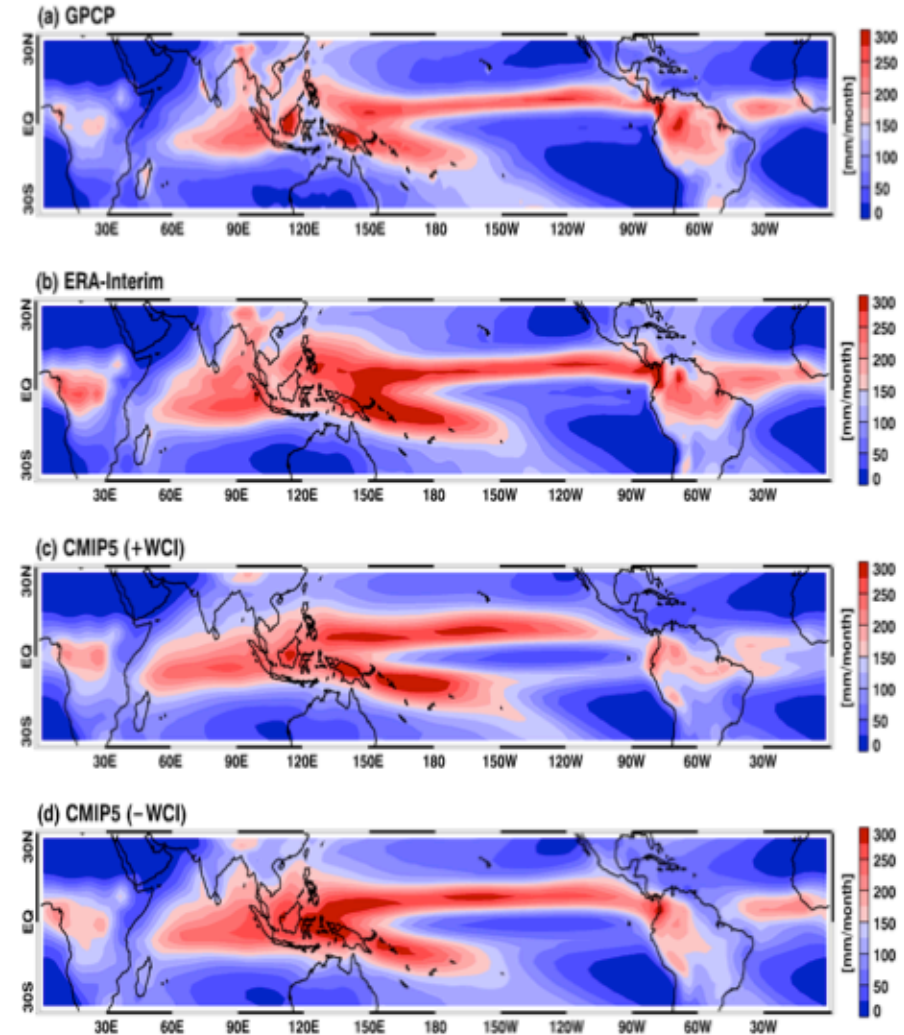


Water vapor transport & Precipitation (Climatology)

Water vapor transport

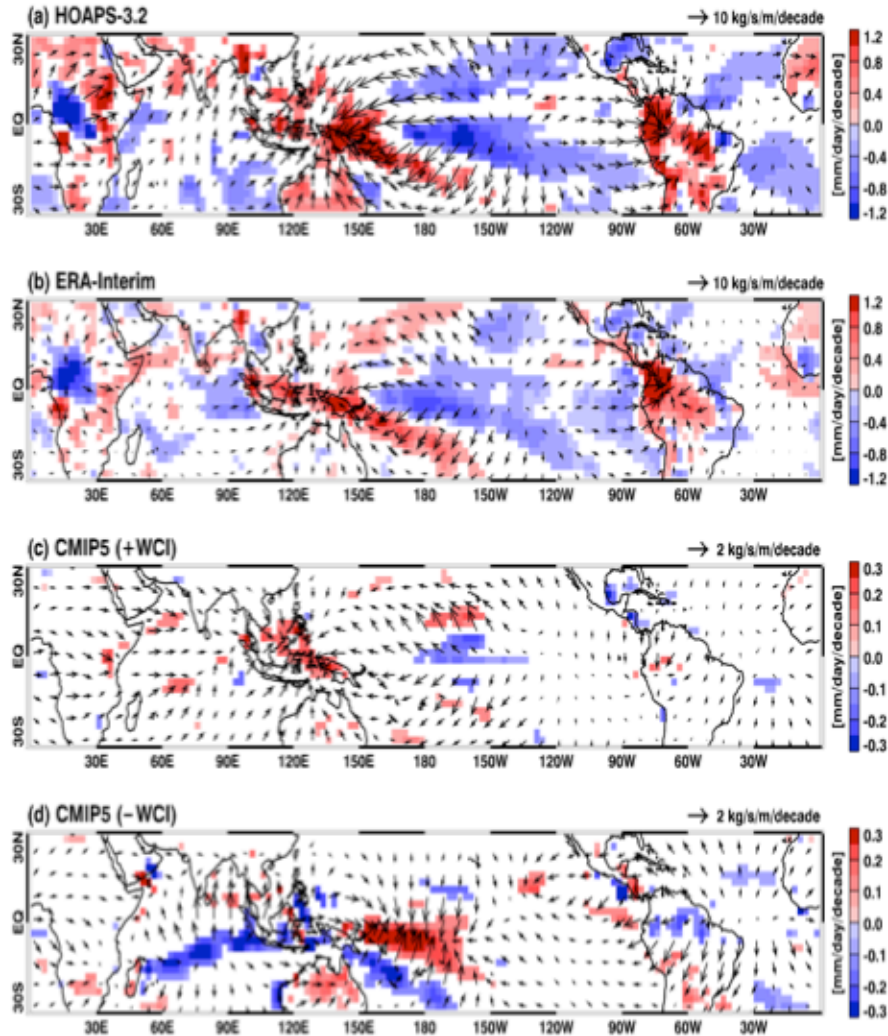


Precipitation

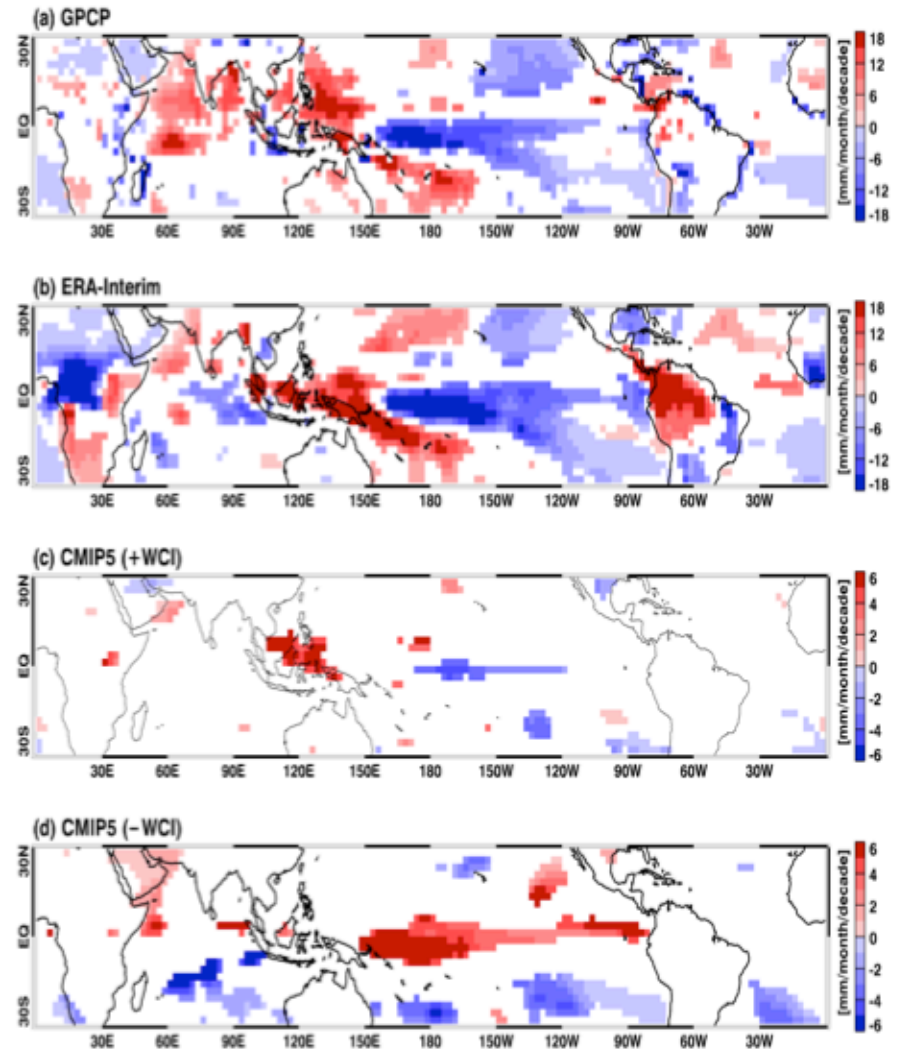


Water vapor transport & Precipitation (linear trend)

Water vapor transport

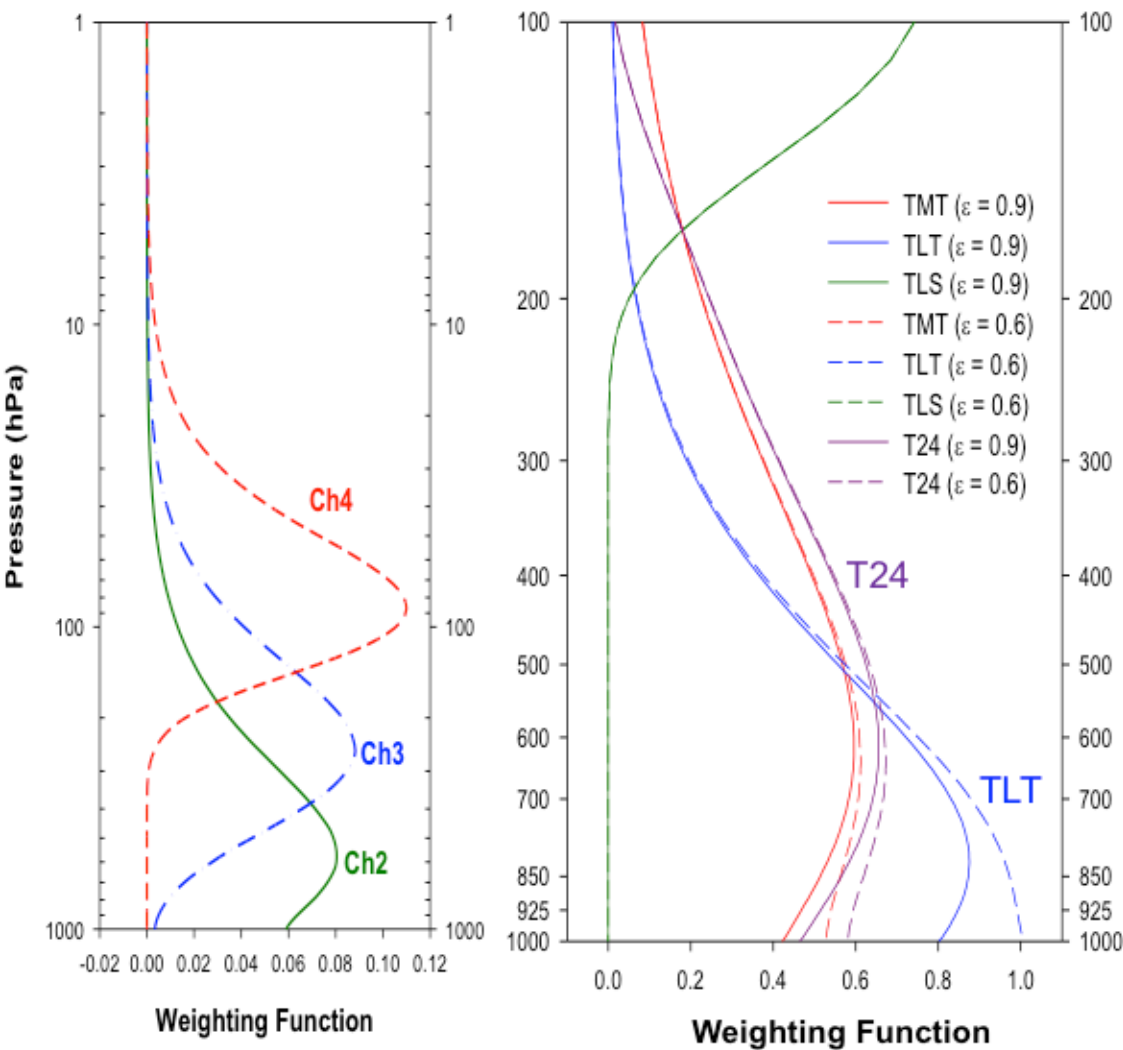


Precipitation



Stability parameter (MSU/AMSU)

MSU/AMSU weighting function (RSS)



- Data

MSU Ch2

: Temperature Middle Troposphere

MSU Ch4

: Temperature Lower Stratosphere

MSU Ch2 (nadir – limb) (TLT)

: Temperature Lower Troposphere

MSU Ch2 + Ch4 (T24)

: Temperature Total Troposphere

($T24 = a \times Ch2 - b \times Ch4$; $a = 1.1$, $b = 0.1$)

- **Period:** 1979-present



T24 - TLT : stability parameter

(Fu et al. 2011)

Surface contribution corrected T24, TLT

$$\text{TOA TB} = \varepsilon_s T_s \tau_s + (1 - \varepsilon_s) \tau_s \int_{\tau_s}^1 T(p) d \ln \hat{t} + \int_{\tau_s}^1 T(p) d \tau$$

TOA TB = surface contribution + atmospheric contribution to TOA

Measured vs. Calculated

To estimate the static stability of the atmosphere, thermal states in the atmosphere are needed, i.e.: atm component of the TOA T24 - TLT.

(1) ATM of MSU/AMSU TOA T24 –TLT:

Measured TOA - calculated surface component

Surface component is calculated with observed SST and ERAI T, q profiles.

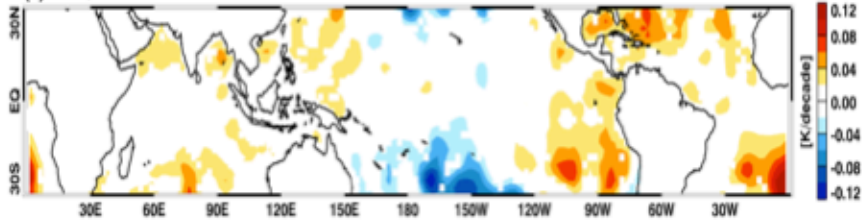
(2) ATM of ERAI, CMIP5 T24 – TLT:

directly calculated from atmospheric T, q profiles

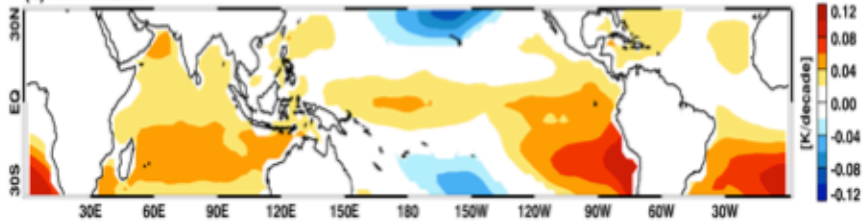
Linear trend of T24 - TLT

TOA T24-TLT

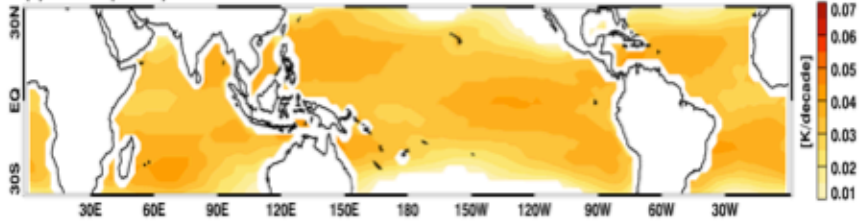
(a) MSU/AMSU



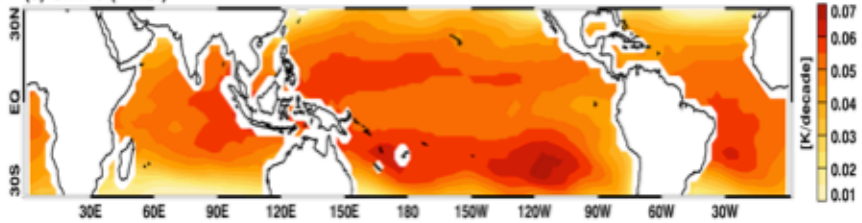
(b) ERA-Interim



(c) CMIP5 (+WCI)

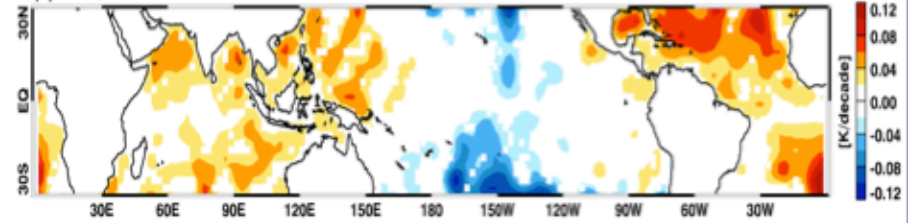


(d) CMIP5 (-WCI)

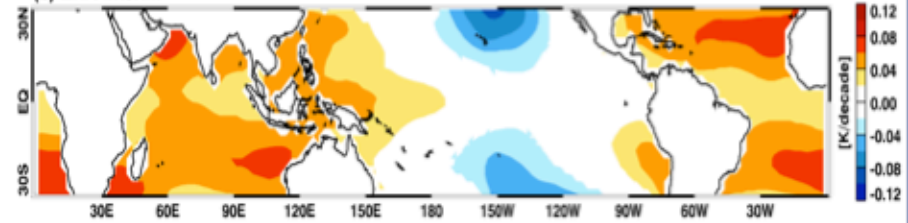


ATM T24-TLT

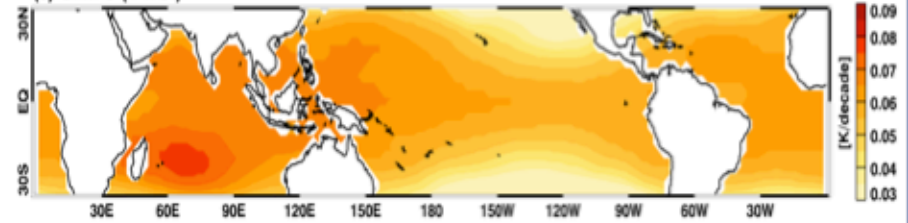
(a) MSU/AMSU



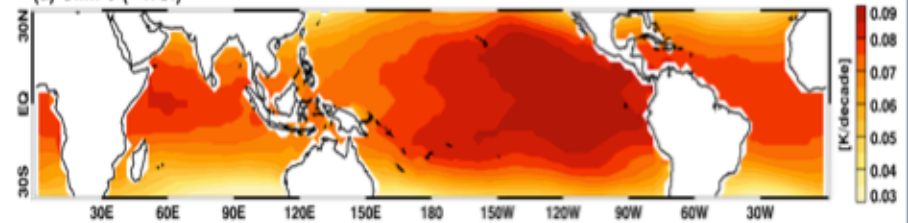
(b) ERA-Interim



(c) CMIP5 (+WCI)



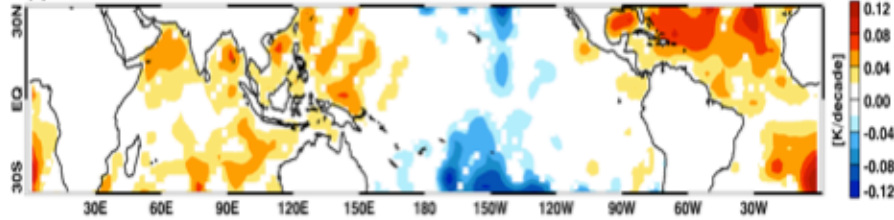
(d) CMIP5 (-WCI)



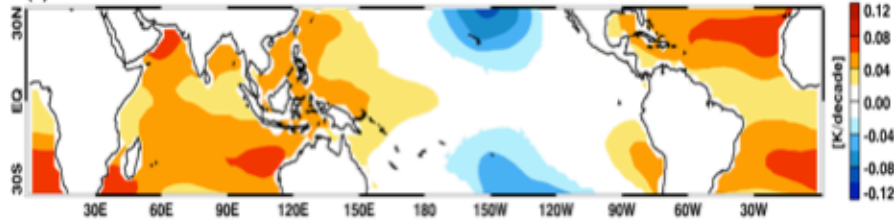
(T24 - TLT) vs. SST/SLP trend

ATM T24-TLT

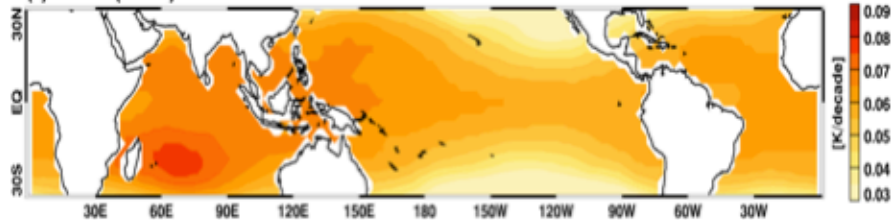
(a) MSU/AMSU



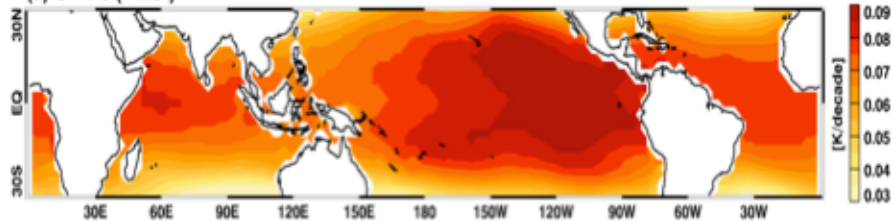
(b) ERA-Interim



(c) CMIP5 (+WCI)

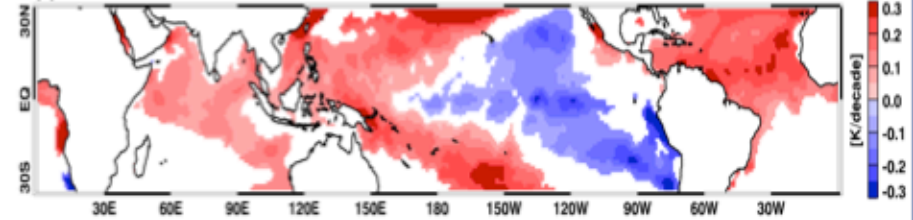


(d) CMIP5 (-WCI)

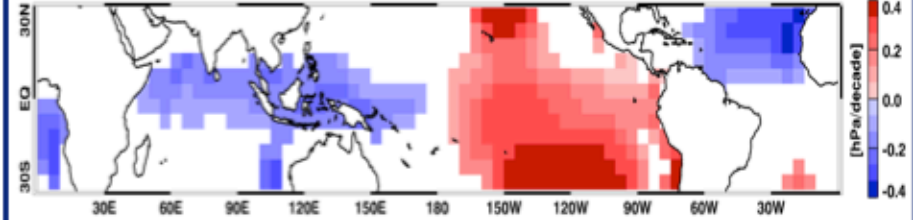


SST/SLP

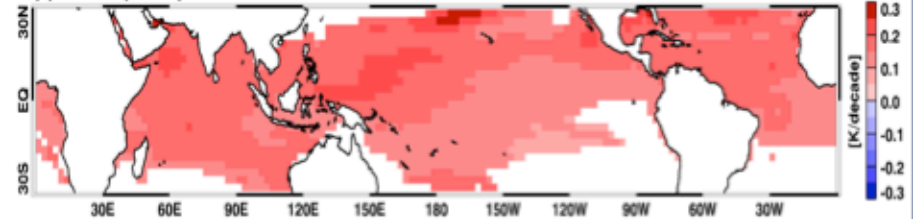
(a) HadISST



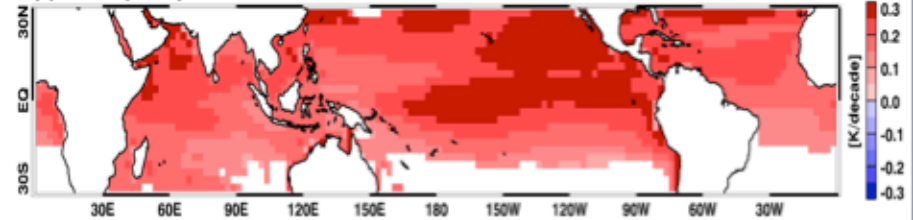
(b) HadSLP2



(c) CMIP5 (+WCI)



(d) CMIP5 (-WCI)



Diabatic heating vs. Dry static stability

Diagnose the relative importance of east-west contrasts in **diabatic heating** vs. **dry static stability** for the Walker circulation variability & trend

The first-order thermodynamic energy balance of large-scale tropical circulation (at any time and location) is between diabatic heating & adiabatic cooling,

$$Q \approx -\omega \times \left(-\frac{T}{\theta} \frac{\partial \theta}{\partial p} \right) \approx -\omega \times (S_p)$$

where Q is the diabatic heating; $S_p = \left(-\frac{T}{\theta} \frac{\partial \theta}{\partial p} \right)$, the static stability parameter, and $\omega = \frac{dp}{dt}$.

$$dQ \approx -d\omega \times S_p - \omega \times dS_p$$

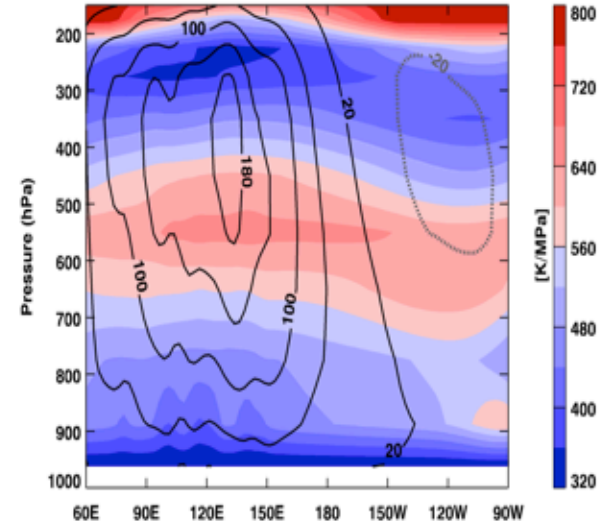
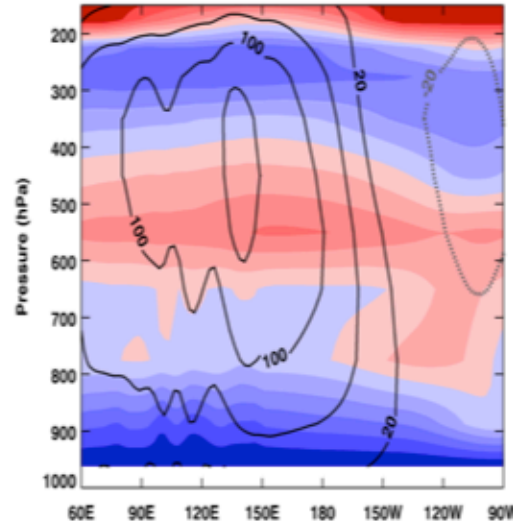
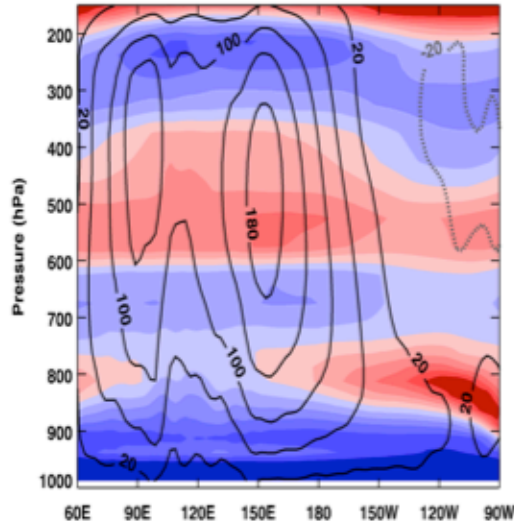
Dry static stability & omega wind (climatology, trend)

ERA-Interim

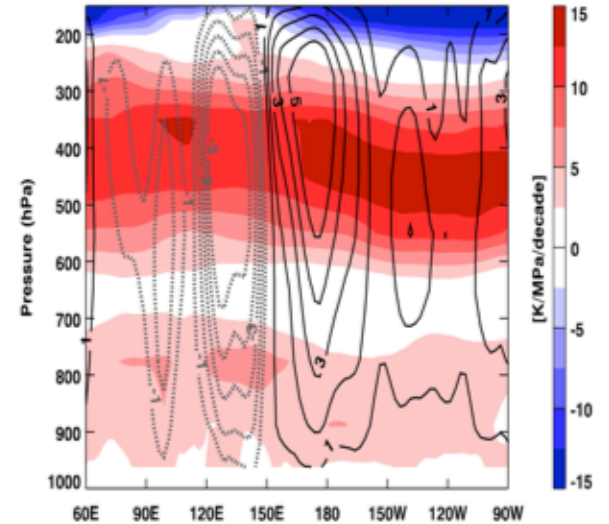
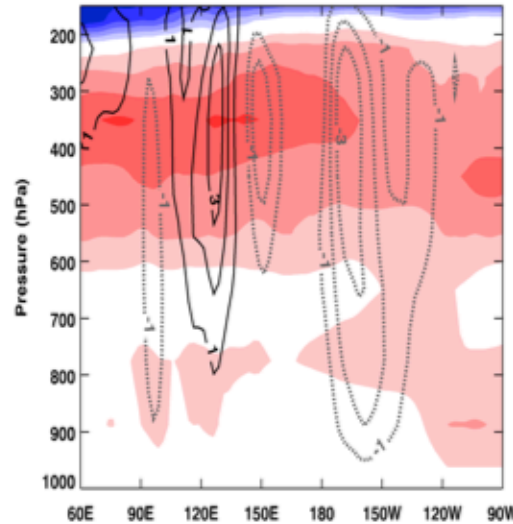
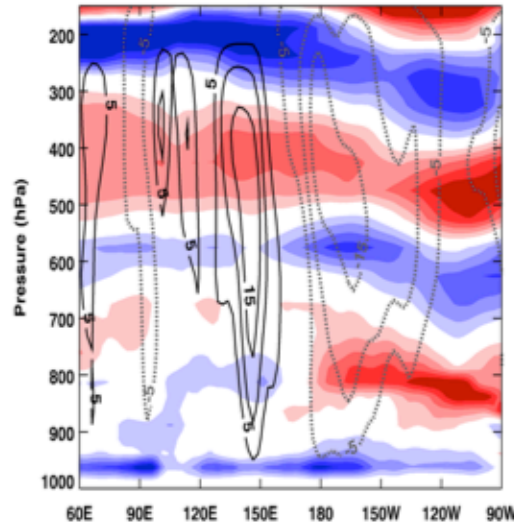
CMIP5 (+PWCI)

CMIP5 (-PWCI)

$\overline{S_p}, -\overline{\omega}$



$\Delta S_p, -\Delta \omega$

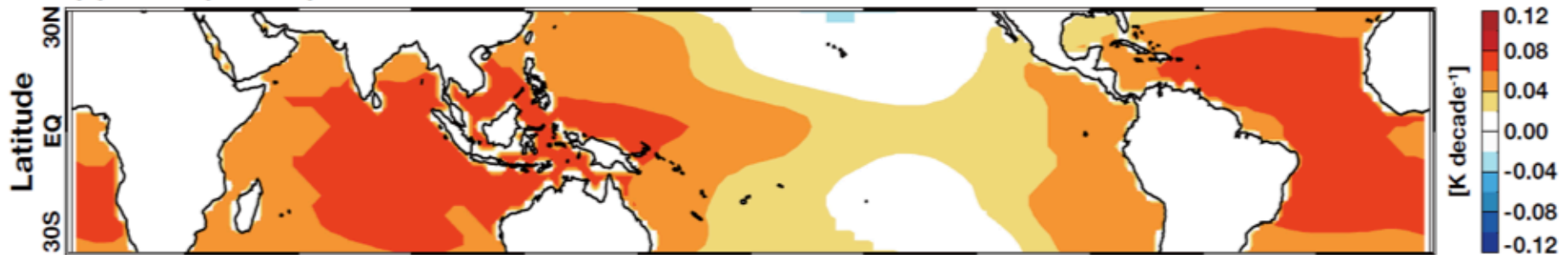


AMIP runs

- We examine the AMIP runs where time-evolving observation-based SST fields are prescribed throughout the model integration.
- Therefore, deviations in the trends in static stability cannot be attributed to differences in SST or atmosphere-ocean interactions, be the differences due to natural variability and/or to model deficiencies.
- There are five +PWCI and five -PWCI models, but only **four +PWCI models** (NorESM1-M, GFDL-CM3, INM CM4, IPSL-CM5A-MR) and **three -PWCI models** (ACCESS1-0, MPI-ESM-MR, MIROC5) were used for the AMIP analysis because the remaining three model outputs are unavailable in the AMIP archive.

AMIP T24-TLT (linear trend)

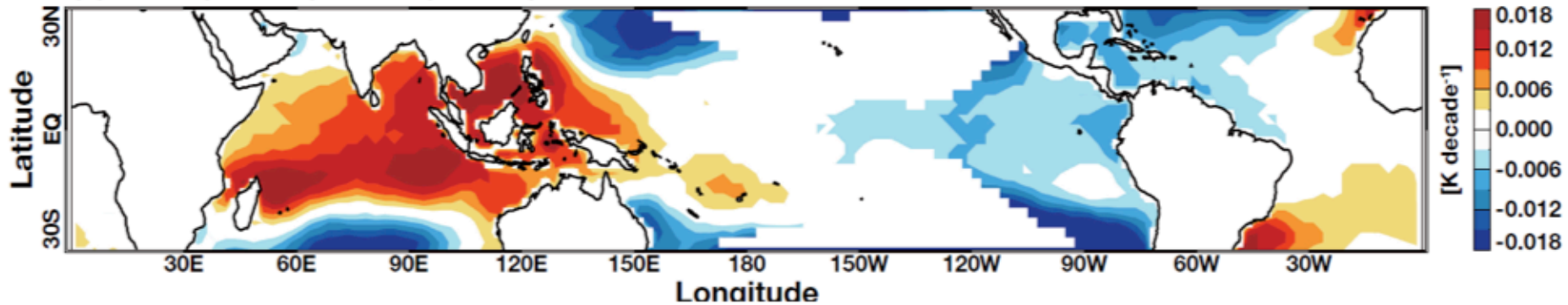
(a) AMIP (+PWCI)



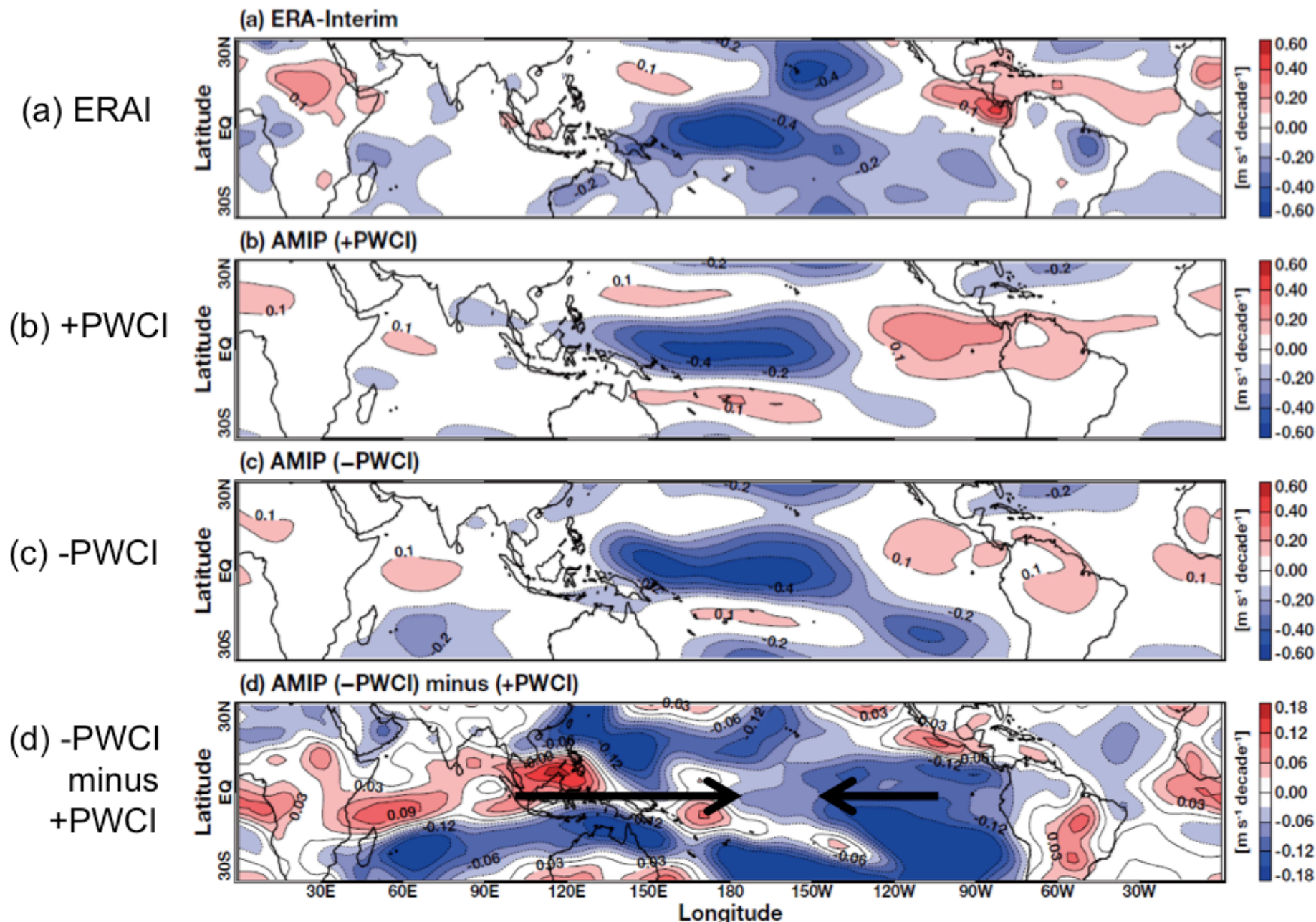
(b) AMIP (-PWCI)



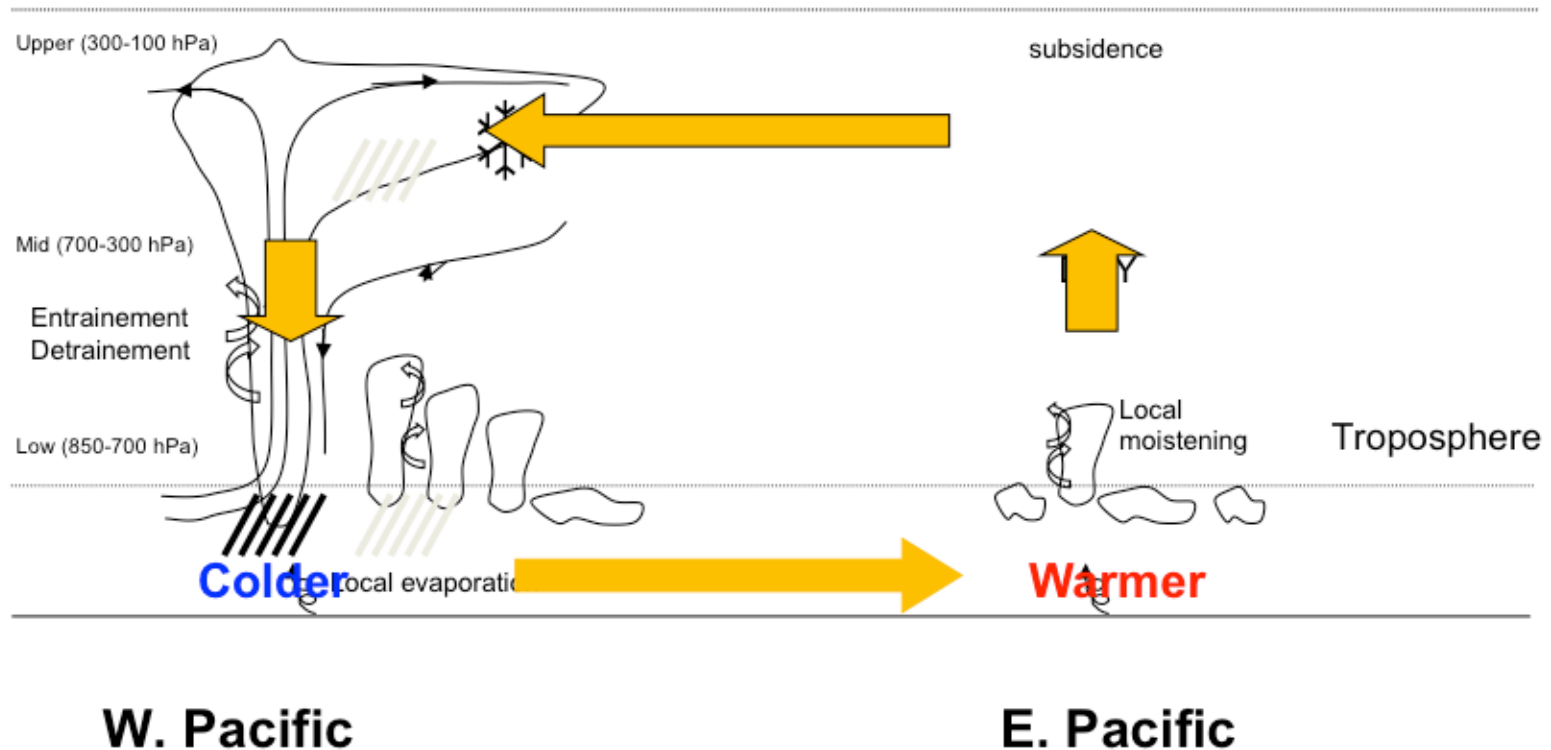
(c) AMIP (-PWCI) minus (+PWCI)



AMIP Near-surface U wind ($U > 0$: eastward)



Role of stability in the weakened Walker circulation (Summary of -PWCI models)



-PWCI model representations of atmospheric static stability can also help explain the El-Niño-like SST trend simulated by the models

Summary

- The static stability trend:
CMIP5 models > ERAI and MSU/AMSU
Among CMIP models: -PWCI > +PWCI
- -AMIP models (even with same observed SST) show greater stabilization over the western tropical Pacific,
and show comparatively eastward acceleration over the tropics.

If the models' ocean is allowed to respond, warm waters from WP would spread to the east. This is consistent with SST trends in -CMIP models.

- Model representations of atmospheric static stability can also contribute to the El-Niño-like SST trend simulated by the models.
- Findings here suggest that improvements in the models' representation of tropical stability, through a better convective parameterization, can help reduce the uncertainty in the strength of the PWC.